Journal of Photochemistry & Photobiology, B: Biology 230 (2022) 112438

Contents lists available at ScienceDirect

Journal of Photochemistry & Photobiology, B: Biology

journal homepage: www.elsevier.com/locate/jphotobiol

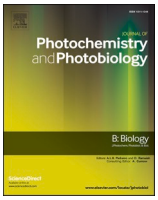

Hemorheological alterations of red blood cells induced by 450-nm and 520-nm laser radiation

Ruixue Zhu [a,*], Tatiana Avsievich [a], Xinyang Su [b], Alexander Bykov [a], Alexey Popov [c], Igor Meglinski [a,d,e,f,g,h,*]

[a] Optoelectronics and Measurement Techniques, University of Oulu, 90570 Oulu, Finland
[b] School of Science, Beijing Jiaotong University, 100044 Beijing, China
[c] VTT Technical Research Centre of Finland, 90590 Oulu, Finland
[d] Interdisciplinary Laboratory of Biophotonics, National Research Tomsk State University, 634050 Tomsk, Russia
[e] Institute of Clinical Medicine N.V. Sklifosovsky, I.M. Sechenov First Moscow State Medical University, Moscow 129090, Russia
[f] REC Fundamental and Applied Photonics, Nanophotonics, Immanuel Kant Baltic Federal University, Kaliningrad 236016, Russia
[g] College of Engineering and Physical Sciences, Aston University, Birmingham B4 7ET, UK
[h] V.A. Negovsky Scientific Research Institute of General Reanimatology, Federal Research and Clinical Center of Intensive Care Medicine and Rehabilitology, Moscow 107031, Russia

ARTICLE INFO

Keywords:
Red blood cells
Low-level laser radiation
Biomodulation
Aggregation
Deformation
Optical tweezers

ABSTRACT

Proper rheological properties of red blood cells (RBC) including flexibility and aggregability are essential for healthy blood microcirculation. Excessive RBC aggregation has been observed to be associated with many pathological conditions and is crucial in acute circulatory problems. Low-level laser radiation (LLLR) has been found to have positive effects on the rheology of human blood, however, the detailed mechanisms of blood photobiomodulation remains unclear. In this study, utilizing the single-cell technique optical tweezers (OT) and traditional light microscopy, the influence of photobiomodulation of human RBC was examined under different conditions of laser irradiation. The results revealed that high radiant exposure (over 170.5 J/cm^2 radiant fluence) caused enhanced RBC aggregation and cell shape transformation while the aggregation force between single RBC remained unchanged. LLLR with radiant fluence below 9.5 J/cm^2 by 450 nm wavelength improved the RBC deformability, weakened the strength of cell-cell interaction in the RBC disaggregation process, and showed rejuvenating effects on RBC suspended in a harsh cell environment.

1. Introduction

Red blood cells (RBC) of healthy human blood are observed to reversibly form clusters termed “rouleaux” in distinctive arrangements resembling stacks of coins at stasis or low-flow-rate conditions [1]. The process of forming two/three-dimensional rouleaux through face-to-face and face-to-edge attachments is termed “aggregation” and the detachment of aggregates is described as disaggregation [2]. Studies have revealed the vital role of proper RBC aggregation in regulating blood viscosity and tissue-organ perfusion [3–5]. Enhanced RBC aggregation has been reported in various clinical conditions including malaria, infections, acute circulatory problems such as myocardial/cerebral ischemia and infarction and peripheral vascular diseases, stable angina, and coronary slow-flow phenomenon [3,6]. However, several basic aspects of RBC aggregation mechanism and dynamics and in vivo effects on blood flow remain unclear and there is an urgent need for methods that can effectively improve the RBC aggregation state, especially in the situations of acute myocardial/cerebral infarctions [7].

For more than four decades, laser biomodulation effects on human blood including modifications in structural and functional properties have been studied in various irradiation protocols with a broad spectral range (ultraviolet, blue, green, red, infrared) and through different irradiation methods such as intravenous and transcutaneous blood irradiation [8]. Positive effects of low-level laser radiation (LLLR) on improving blood microcirculation, inducing anti-inflammatory effects, stimulating the immune response, normalizing blood rheology, and reducing infarct size in acute myocardial infarction have been reported [8–10]. Most in vitro studies that investigated the laser irradiation

* Corresponding authors at: Optoelectronics and Measurement Techniques, University of Oulu, 90570 Oulu, Finland.
E-mail addresses: ruixue.zhu@oulu.fi (R. Zhu), i.meglinski@aston.ac.uk (I. Meglinski).

https://doi.org/10.1016/j.jphotobiol.2022.112438
Received 30 January 2022; Received in revised form 21 March 2022; Accepted 25 March 2022
Available online 29 March 2022

effects on the rheological properties of blood cells especially of RBC were based on traditional analyzing methods and statistical results on a macroscale were obtained. For instance, RBC deformation is evaluated based on the performance of a large number of cells in red cell deformability meter, RBC aggregation degree is typically assessed by the erythrocyte sedimentation rate (ESR) measurement based on Wintrobe tubes, and zeta potential is analyzed by electrophoretic mobility [11–13]. Furthermore, the irradiation of the blood sample was typically done in test tubes with a larger diameter than the beam spot, so the blood sample need to be continuously stirred [14] or only a fraction of the blood surface was irradiated directly [11,13]. Such irradiation methods will somehow affect the experimental observation of the biomodulation effects of LLLR, and the reported effective radiant exposure varied from 0.27 J/cm^2 to 550 J/cm^2 in different studies [10,12,13]. Moreover, the detailed modulation mechanism of LLLR on RBC behavior and cell properties remains in discussion, and more studies are needed for a better understanding of laser biomodulation effects and for thoughtful designing of the irradiation protocol.

Optical tweezers (OT) is served as the single-cell manipulation method to study the effects of LLLR on the rheological properties of RBC in vitro. The optical trapping phenomenon based on radiation pressure is derived from the fact that light carries momentum [15]. As a Nobel-prize winning technique, OT has a profound impact on cell biology and bio-nanotechnology research and has become a vital tool in hemorheology studies [2,16]. With the ability to non-invasively manipulate single cells with controllable trapping forces, OT can reveal the microscopic mechanisms under the cell membrane deformation and intercellular interaction and communication among RBC at the pico-Newton level [17]. The aim of the current study was to explore the biomodulation effects of laser irradiation on the in vitro rheological properties of human RBC including spontaneous aggregation at rest, cell deformability, dis/aggregation dynamics, and survival of RBC in the harsh environment by conventional light microscopy and OT. The modulation mechanism of laser irradiation on the RBC mutual interaction dynamics was revealed for the first time at the single-cell level.

2. Materials and Methods

As the single-cell level measurement by OT is very sensitive to external influences, the blood samples utilized in the current study were donated by one healthy donor (female, age 28) with oral consent and under the ethical permission (Finnish Red Cross, No. 7/2021) to avoid donor-specific differences. The standard erythrocyte sedimentation rate (ESR) of the donated blood was measured at a Mehiläinen clinic (Oulu, Finland) as 2 mm/h within the normal range (≤ 20 mm/h). The experimental samples were prepared by diluting washed RBC from finger-prick blood in platelet-free autologous plasma obtained from double-centrifuged whole blood (hematocrit <1%). The prepared blood sample was injected into a sample chamber consisting of a microscopic slide and a cover glass bonded by double-sided tapes (100 μm thick) for irradiation treatment and following studies. The inner thickness (i.e., the distance between the bottom and upper glass surfaces) of the sample chamber was measured to be about 70–80 μm. The detailed instructions on sample preparation can be found in our previous studies [18,19]. The irradiation treatment was applied by localizing the sample chamber on the irradiation stage of the in-house made laser irradiation platform as shown in Fig. 1(a). Continuous diode lasers (Oxlasers, China) with measured beam diameters of about 11 mm as shown in Fig. 1(b) were used as irradiation sources. According to the First Law of Photochemistry, the premise of photochemical reaction is that photons are absorbed by molecular photoreceptors or chromophores [20]. The irradiation wavelength of 450 nm close to the highest absorption peak of the targeted photoreceptor (i.e., hemoglobin) according to the hemoglobin absorption spectra as shown in Fig. 1(c) was adopted. The 520-nm wavelength, which can be absorbed by hemoglobin but has a lower absorption coefficient than the 450-nm wavelength, was selected for comparison. A triangular-shaped prism with experimentally measured light transmission efficiency (P_{out} / P_{in}) of about 90% for both 450- and 520-nm wavelength was used to direct the laser beam to the sample chamber. The irradiation power was measured below the prism at the sample stage. The output power of the diode lasers is stable enough for our experiments as the relative fluctuations in the output power were measured to be 0.4% and 5% for 450- and 520-nm wavelengths after 3 h of operation at room temperature. The microscopic cover glasses used to make the sample chambers are made of high transmittance glass, thus the absorption by cover glasses was ignored. The temperature drift on the surface of the sample chamber was measured to be no more than 0.3 °C for up to 4 h irradiation with a maximum output power of 50 mW by both wavelengths. For the given wavelength, the radiant fluence or exposure (H_e) is the radiant energy (Q_e) received by per unit area (A) and is calculated by:

$$H_e = \frac{Q_e}{A} = \frac{\Phi_e \bullet t}{\pi \bullet r^2} \ (\mathrm{J/cm2}) \quad (1)$$

where Φ_e is the radiant flux/power (W), t is irradiation time (s), and r is the radius of the irradiated area (5.5 mm). Only the cells in the sample chamber within the irradiation area covered by the laser beam were

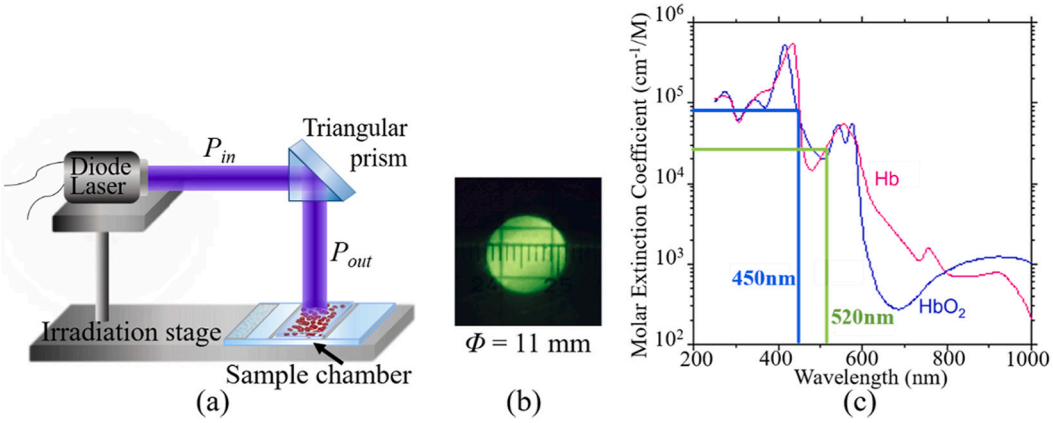

Fig. 1. (a) Schematic layout of the sample irradiation platform made of a continuous-wave diode laser and a triangular prism with a light transmission efficiency (P_{out}/ P_{in}) of about 90% for both 450- and 520-nm wavelength. (b) The diameter of the irradiation beam is measured to be 11 mm. (c) Absorption spectra of oxy- and deoxy-hemoglobin (HbO_2 and Hb) with blue and green lines indicating the wavelengths (450 and 520 nm) used for blood sample irradiation. Reproduced from Prahl S. Optical Absorption of Hemoglobin. Copyright © 1999 Prahl S. Available from: https://omlc.org/spectra/hemoglobin/. (For interpretation of the references to colour in this figure legend, the reader is referred to the web version of this article.)

studied. The irradiation conditions used in the experiments are named in the form of "wavelength_power".

An Eclipse LV100DA-U microscope (Nikon, Japan) was used to observe the RBC spontaneous aggregation process after a certain standing/irradiation time. The dual-trap OTs system used to manipulate RBC to study the cell deformation and cell-cell interaction is schematically sketched in Fig. 2(a). The main components are an infrared (λ = 1064 nm) Nd:YAG trapping laser source (ILML3IF-300 Leadlight Technology, China), two polarizing beam splitters to split the laser beam into two channels, and a water immersion objective with a high numerical aperture (LUMPlanFl 100×/1.00 W, Olympus, Japan) to form gradient force traps. It has been well manifested in our previous studies that the continuous trapping of RBC within the infrared optical traps with the trapping power of less than 100 mW for up to 5 min will not affect the rheological properties of trapped RBC [2,18,21]. In the current study, the trapping wavelength of 1064 nm is in the low absorption spectral range of hemoglobin and each measurement by OT was performed within 1 min with trapping power below 70 mW, therefore, the trapping laser was not supposed to influence the measured RBC rheological properties. The trapped RBC was observed to align with the polarization direction of trapping beams as shown in Fig. 2(b). The relationship between the laser power and the trapping force was calibrated with the method used in our previous studies [2,18] and the result is shown in Fig. 2(c). The laser power represents the output laser power measured after the "beam expander" module before being directed to the objective. All measurements were carried out at room temperature (23 ± 1 °C).

3. Results

3.1. Laser Irradiation Effect on RBC Spontaneous Aggregation Studied by Conventional Light Microscopy

As one of the most important determinants of blood rheology and microcirculation, the intrinsic and well-known property of RBC in forming binding structures "aggregates" or "rouleaux" by attaching to each other was examined by conventional light microscopy. The samples were observed under a 20 × objective after a certain standing (control sample) or irradiation time. At least 20 microscopic images were taken and the number of single RBC and all objects, as well as the sizes of the RBC aggregates, were counted and analyzed to evaluate the effect of laser irradiation on the process of rouleaux formation and to select proper irradiation conditions for further studies. For the control sample, Fig. 3 illustrates the changes in the status of RBC in the prepared sample over time. The column chart in Fig. 3(a) shows the changes in counts of total objects and aggregates with the line chart better indicates the trend of the changes. Fig. 3(b) presents the lognormal distributions of the sizes (areas) of RBC aggregates with the rug plot visualizes the distribution of the discrete data. It can be concluded that not only the total number but also the size of aggregates increased gradually while the number of total objects decreased with time. The results demonstrate that in the in vitro experimental condition, the RBC suspended in the autologous platelet-free plasma intrinsically clump together to form aggregates that follow a lognormal distribution and become larger over time.

For the irradiated samples, up to 180 min irradiation by 520-nm laser operated at a maximum of 50 mW did not cause any morphological changes to the blood samples. A normal morphology of individual cells and cell aggregates is shown in Fig. 4(a). However, obvious cell distortion appeared after 90-min irradiation by 450-nm laser operated at 50 and 30 mW, as illustrated by Fig. 4(b). Irradiation by 450-nm laser operated at lower power (e.g., 15 mW) for longer time (e.g., 180 min) also caused similar morphologic changes, which did not recover after irradiation stopped. Therefore, high radiant exposure (over 170.5 J/cm^2) by 450-nm wavelength caused irreversible morphological damage to RBC. In the low radiant exposure irradiation groups of "450nm_5mW", "450nm_15mW", and "450nm_30mW", the normalized total counts (normalized to t = 0 min) of spontaneously formed aggregates after different standing/irradiation time were compared as shown in Fig. 5. The counts of aggregates increased rapidly in the irradiation groups with time and far exceeded the count in the control group after 30 min of irradiation. Enhanced formation of RBC aggregates was also observed in the high radiant exposure irradiation groups of "450nm_50mW" and "520nm_50mW" as shown in Fig. 6. Furthermore, the normalized average values and the lognormal distribution of the size (area) of formed aggregates were compared between the control and different irradiation groups as shown in Fig. 7. In both the low and high radiant exposure groups, though there is little difference in the average size of formed aggregates, the distribution curves obviously expanded to large size areas (i.e., more large aggregates appeared) in the irradiated samples. As a conclusion, laser irradiation, especially over 9.5 J/cm^2, speeded up the formation of RBC aggregates and promoted the formation of large aggregates in the spontaneous aggregation process of RBC suspension in the autologous plasma at rest. Therefore, the subsequent investigations of laser irradiation effects on RBC were carried out with low-exposure irradiation below 9.5 J/cm^2 (i.e., by 450 nm laser at 5 mW for up to 30 min).

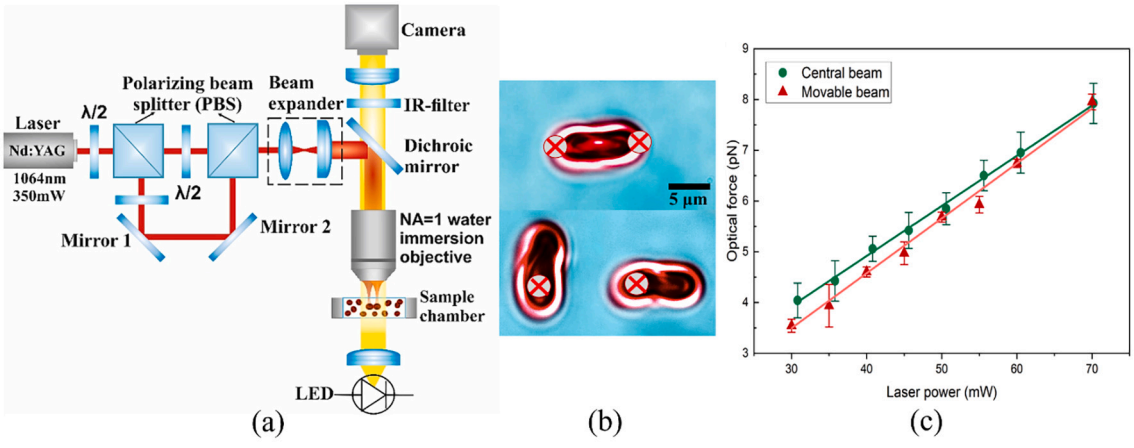

Fig. 2. (a) Illustration of the experimental setup of the OT system comprises an infrared laser source, polarizing beam splitters, focusing objective, a CMOS camera, and other necessary optical components. (b) The colored microscopic images showing the single-cell trapping at two diametrically opposite points (top picture) and by each beam individually (bottom picture). (c) Calibration results for the central (green dots) and movable beams (red triangles). (For interpretation of the references to colour in this figure legend, the reader is referred to the web version of this article.)

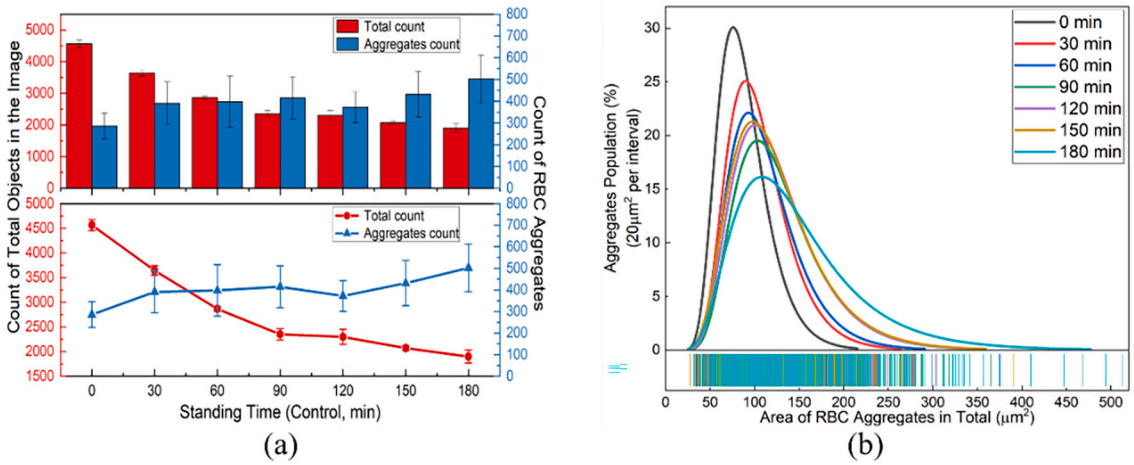

Fig. 3. Results of spontaneous aggregation in the control sample within 180 min. (a) The total counts of all cell objects (red) and of RBC-aggregates solely (blue) in 20 recorded micrographs. (b) Statistical size distributions of RBC-aggregates. (For interpretation of the references to colour in this figure legend, the reader is referred to the web version of this article.)

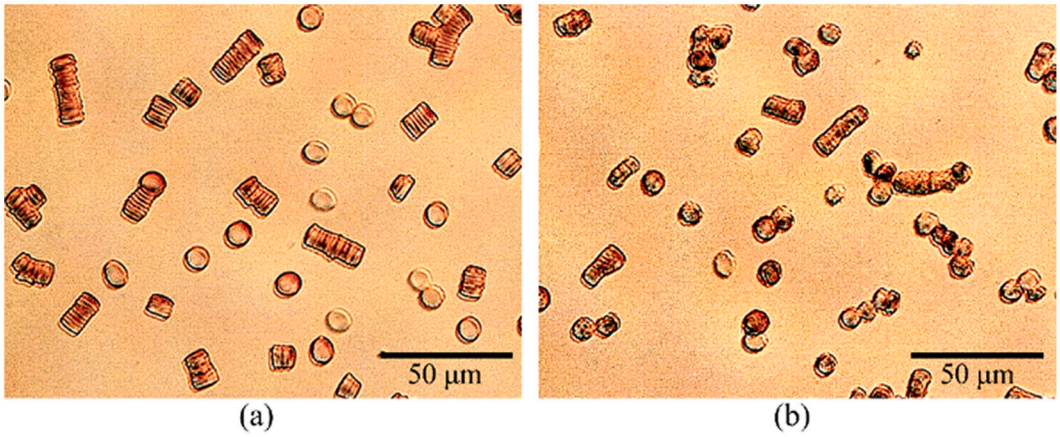

Fig. 4. Illustration of (a) morphology of individual RBC and RBC-aggregates under the observation by conventional light microscope (20 × objective) and (b) morphological changes induced by long time radiation with 450-nm laser.

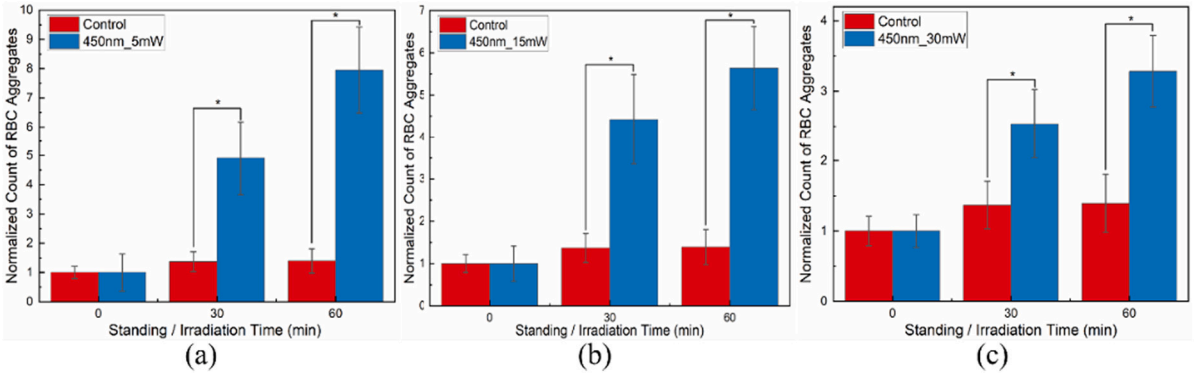

Fig. 5. Comparison between normalized total counts of RBC aggregates in control and low radiant exposure irradiation groups of (a) "450nm_5mW", (b) "450nm_15mW", and (c) "450nm_30mW" for 0, 30, and 60 min of standing/irradiation time. The asterisks denote statistical significance (Mann-Whitney *U* test, $p < 0.05$).

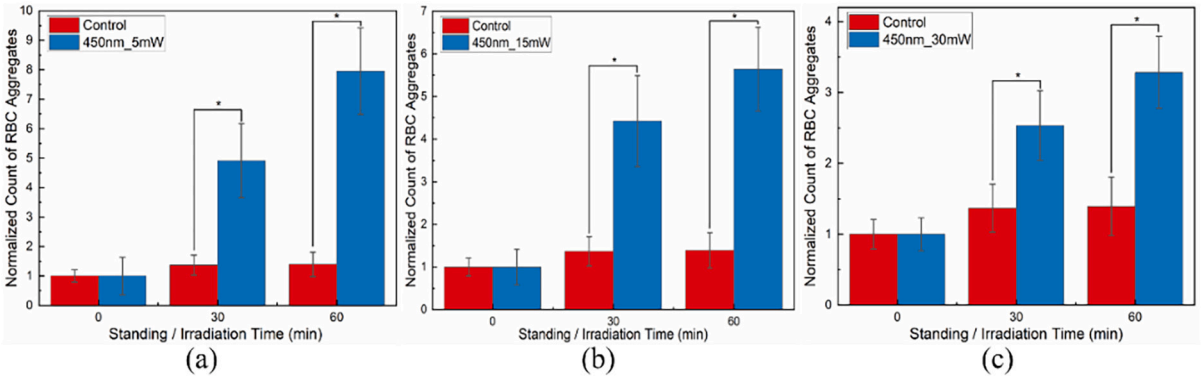

Fig. 6. Comparison between normalized total counts of formed RBC aggregates in control and high radiant exposure irradiation samples of (a) "450nm_50mW" and (b) "520nm_50mW" for up to 180 min.

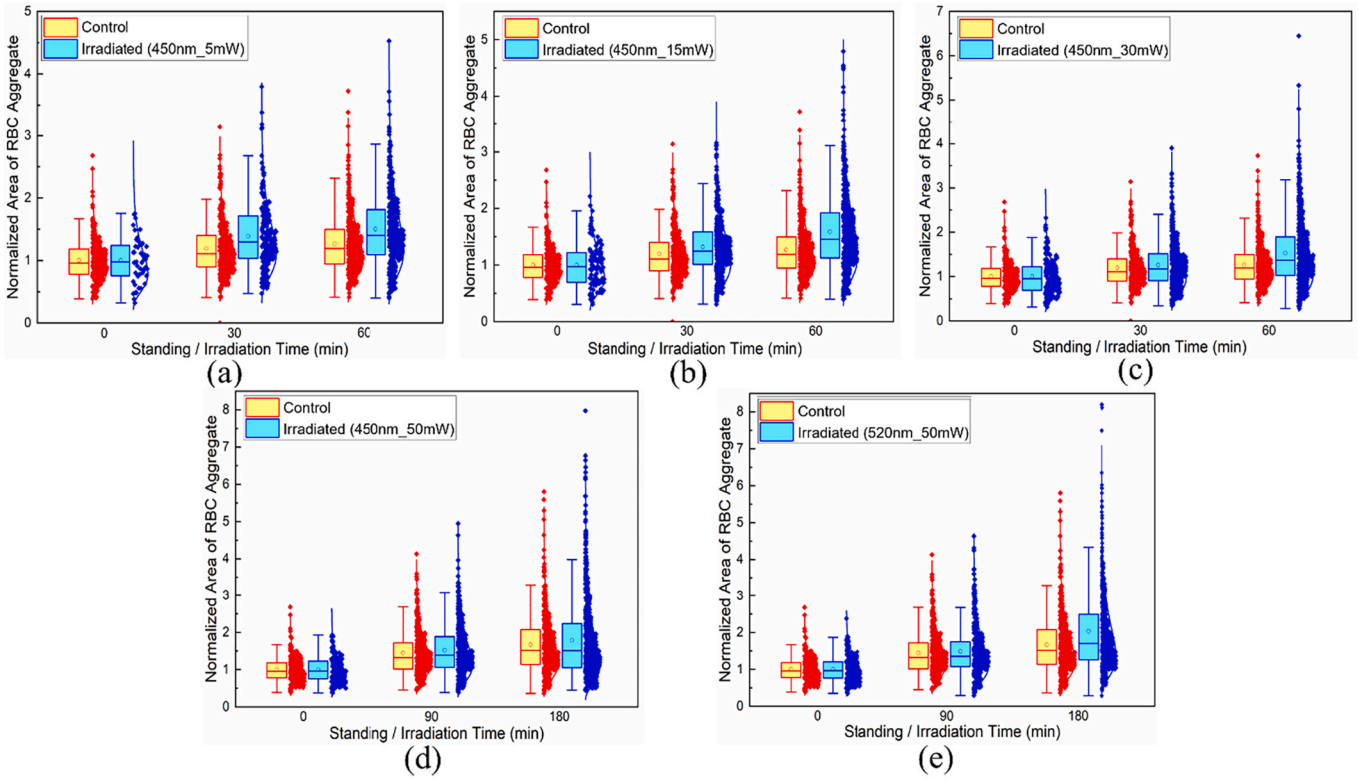

Fig. 7. Comparison of the normalized average values and the lognormal distribution of the size (area) of formed RBC aggregates between the control and different irradiated samples of (a) "450nm_5mW", (b) "450nm_15mW", (c) "450nm_30mW", (d) "450nm_50mW", and (e) "520nm_50mW".

3.2. Laser Irradiation Effect on RBC Aggregation

The aggregation force between two RBC, considered as the force attracting two cells to clump together to form tightly attached aggregate (rouleau) through face-to-face interaction, was studied by OT as the minimum optical holding force to prevent the RBC clumping action from a certain existing contact area between two cells. Experimentally, two individual cells were captured by two trapping beams with sufficiently high power to manipulate the two cells to form a stable initial contact. The power of trapping beams was decreased slowly with the fine adjustment of the relative position between the two traps to keep the contact area between the two cells unchanged. The minimum trapping power that can prevent the cells from aggregating was recorded when cell interaction pulled the RBC out of the traps. With the trapping force calibration results shown in Fig. 2(c), the obtained RBC aggregation force increased almost linearly with the increase of relative initial contact between the two cells as shown in Fig. 8(b). The Pearson correlation coefficient (Pearson's r) was calculated to be 0.768, with the R-Square (R^2) value to be 0.575 in the linear fitting. The contact area between two cells was calculated as the sum of the two segments enclosed by two circular arcs as shown in Fig. 8(a) and the relative initial contact area between RBC was calculated as the ratio of interaction area (S_i) to single-cell surface area (S_0):

$$\frac{S_i}{S_0} = \frac{\sum_{(n=l,r)} \left\{ r_n^2 \left[2 \bullet arccos\left(\frac{r_n - x/2}{r_n}\right) - sin\left(2 \bullet arccos\left(\frac{r_n - x/2}{r_n}\right)\right)\right]\right\}}{(\pi r_l^2 + \pi r_r^2)} \quad (2)$$

where r_l and r_r are the radii of RBC on the left and right sides and x is the length of overlap between the two cells.

Despite of the data fluctuation in Fig. 8(b), the applicability of the

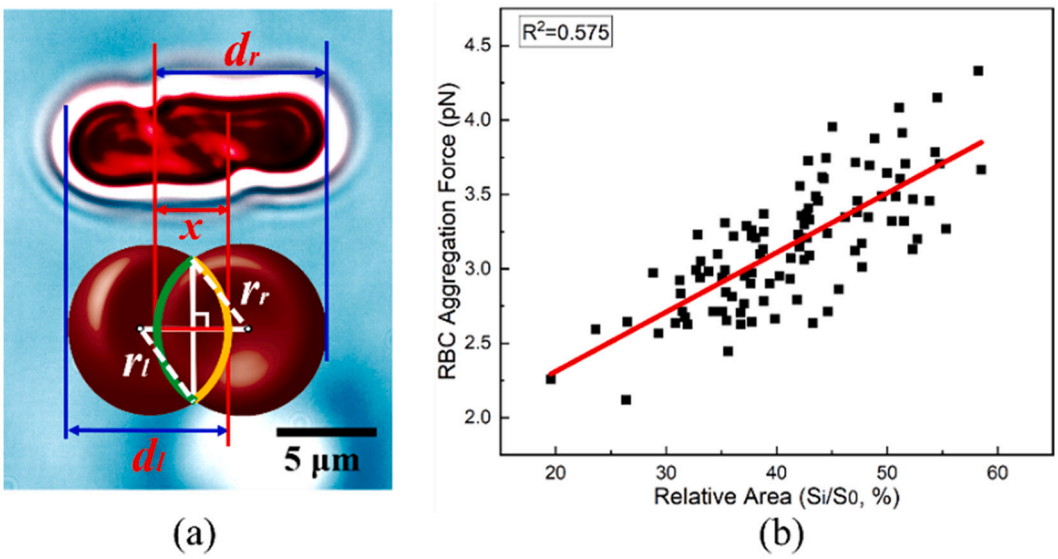

Fig. 8. (a) Illustration of a top-view observation (upper image) and a side-view geometric relationship (lower image) of the cell overlapping that can be calculated as the area within two circular arcs shown in green and yellow. Cell diameters (d_l, d_r) and overlapping length (x) can be extracted from experimental observation. (b) Experimental results of RBC aggregation force (pN) versus relative interaction area in a range of 20% to 60% with a linearly fitting result (red line). (For interpretation of the references to colour in this figure legend, the reader is referred to the web version of this article.)

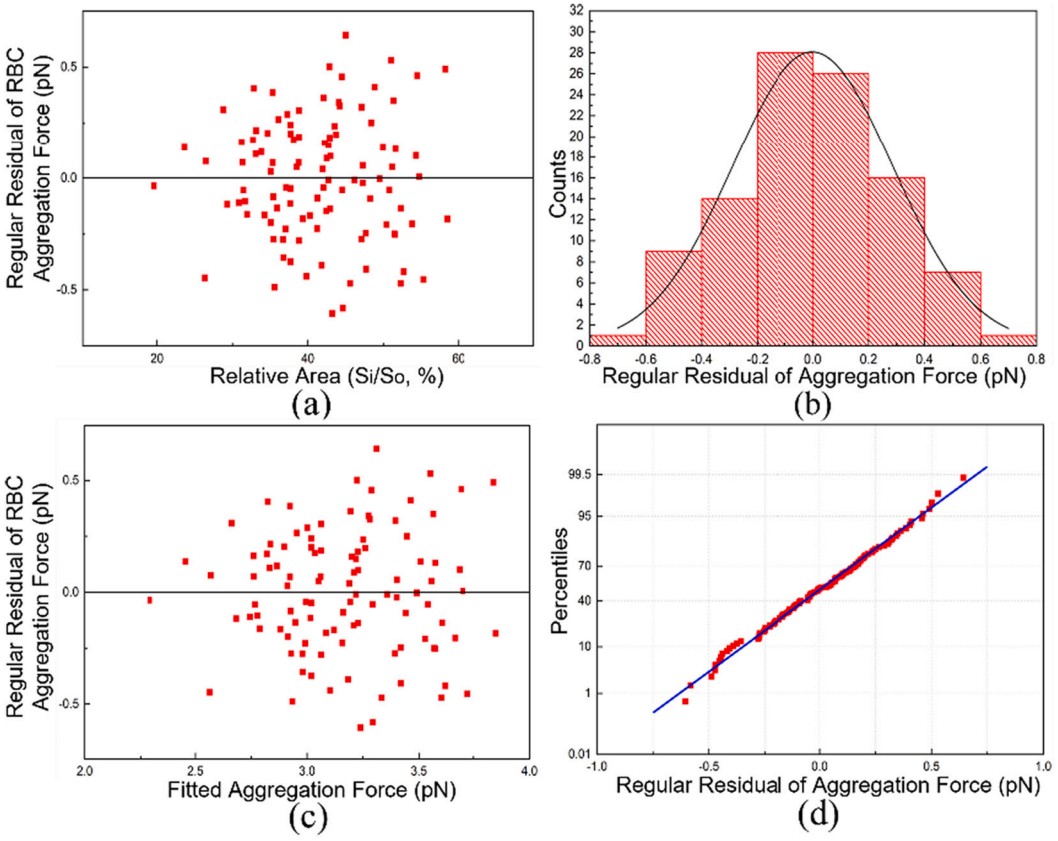

Fig. 9. Statistical analysis of the fitting result of RBC aggregation force. (a) The plot of residuals versus independent variable of relative interaction area. (b) The histogram of the residuals with Gaussian fit. (c) The plot of residuals versus predicted values of RBC aggregation force. (d) The normal probability plot of residuals.

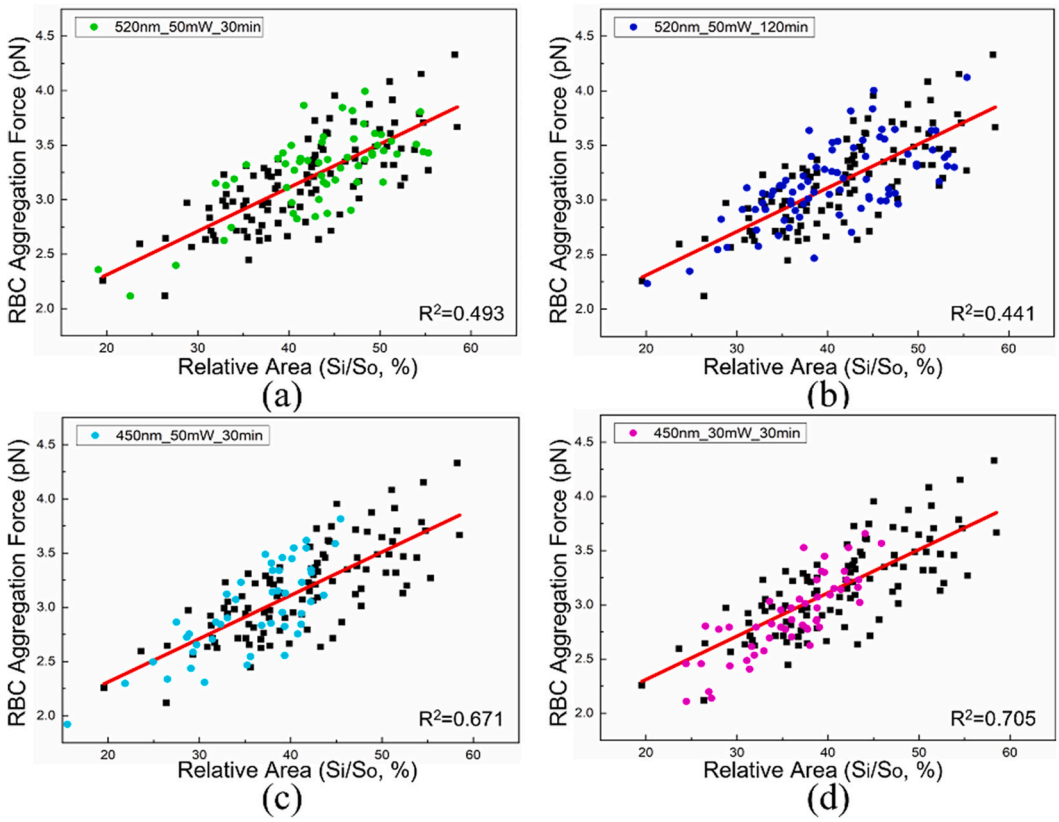

Fig. 10. The comparison between the experimental results of aggregation forces measured in the control group (black dots) and high-radiant-fluence irradiation groups of "520nm_50mW_30min" (green dots), "520nm_50mW_120min" (blue dots), "450nm_50mW_30min" (cyan dots), and "450nm_30mW_30min" (magenta dots). (For interpretation of the references to colour in this figure legend, the reader is referred to the web version of this article.)

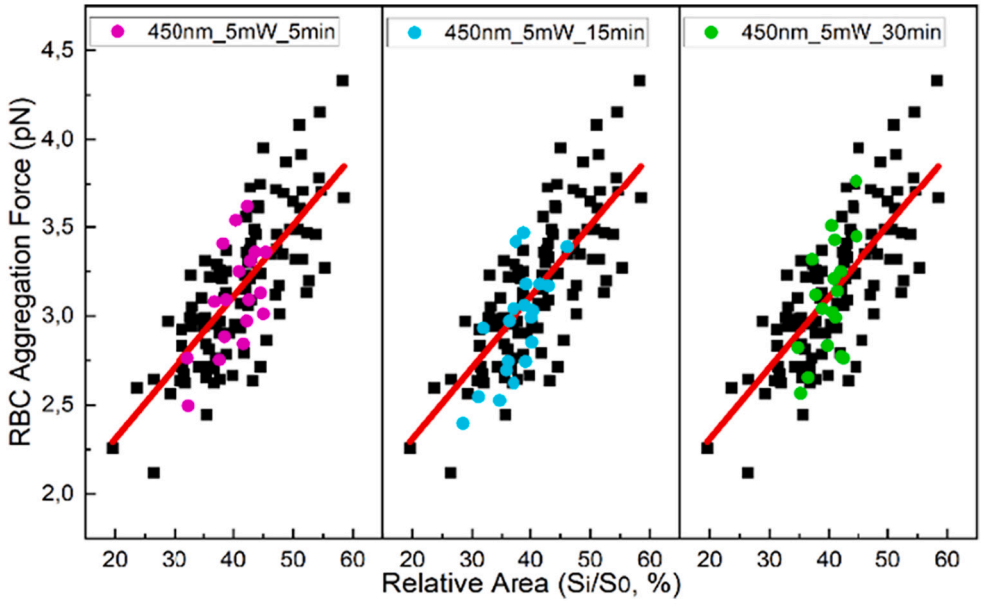

Fig. 11. Comparison of the results of aggregation force measured in the control sample (black dots) and samples irradiated by 450-nm laser operating at 5 mW for 5 min (magenta dots), 15 min (cyan dots), and 30 min (green dots) separately. In the irradiated samples, the RBC aggregation force was mainly measured with an initial relative interaction area of around 40%. (For interpretation of the references to colour in this figure legend, the reader is referred to the web version of this article.)

linear fitting in the experimental data of RBC aggregation force is proved by Fig. 9 with plots of statistical analysis of the linear fitting results. The scatter plots in Fig. 9(a) and (c) show that the residuals of RBC aggregation force against the relative area (S_i/S_0) and the fitted result are disorderedly distributed in an almost horizontal-band pattern, thus the residuals have constant variance. Intuitively, the histogram plot of the residuals Fig. 9(b) exhibits a symmetric bell-shaped distribution around zero and the normal probability plot of the residuals Fig. 9(d) shows a good linear relationship, indicating that the deviation is normally distributed. Therefore, the residual plots prove the validity of the linear fitting model used for the RBC aggregation force analysis.

The RBC aggregation force after irradiation treatment was measured in the same way as in the control group to explore whether the cell interaction was promoted. The RBC aggregation force measured in different high-radiant-fluence irradiation groups are shown in Fig. 10 and the results of different low-radiant-fluence (below 9.5 J/cm^2) irradiation groups are shown in Fig. 11. The low-level-laser irradiation was performed by 450 nm laser operated at 5 mW for up to 30 min, and the aggregation forces were mainly measured around a 40% relative interaction area to simplify the measurement procedure. Compared to the aggregation force measured in the control group, neither high-level nor low-level laser radiation affected the RBC aggregation force.

3.3. Influence of Laser Irradiation on RBC Deformation

RBC are highly deformable and are frequently deformed within the blood flow in blood vessels [22]. RBC can be distorted into axisymmetric parachute shapes or asymmetric slipper-like shapes during circulation depending on the diameters of the capillaries and the direction of pressure gradient within the blood flow [23]. Regardless of the complexity of the actual deformation of RBC in blood vessels, linear stretching of RBC under the action of one-dimensional axial pulling force before and after irradiation was studied by OT. Experimentally, captured RBC was trapped by the dual beams at both ends and placed in the horizontal direction, and was then stretched until the resilience of the cell membrane exceeded the dragging force and pulled the cell out of the trap as shown in Fig. 12. The lengths of the cell before and after optical stretching are denoted by d_o and d_a and the relative stretching is described by the ratio of length change to original length as ($|d_a - d_o| / d_o$) %. The stretching was repeated with several optical pulling forces and the results obtained in the control and low-level laser irradiated samples (by 450 nm laser at 5 mW for 5, 15, and 30 min) were compared as shown in Fig. 13. The cells were elongated with the increase of optical stretching force linearly, and in some conditions the tested cells reached the elongation limit when the relative stretching stopped increasing. From the results in Fig. 13, it is obvious that the deformability of RBC was improved by 450 nm laser irradiation for 15 and 30 min at 5 mW, corresponding to radiant fluence of 4.7 and 9.5 J/cm^2, as the relative stretching increased under the same pulling forces with very small standard deviations. The large standard deviations in Fig. 13(a) reflect that the improvement of cell deformability is not obvious with 5 min irradiation.

3.4. Laser Irradiation Effect on RBC Disaggregation

The RBC disaggregation is considered as the process of enforced separation of two cells initially clumped together. The interaction mechanism and theoretical model of RBC disaggregation are usually described by the "bridging model" and are different and more complex compared with the aggregation process [24,25]. The disaggregation force, which is considered as the external force required to separate individual cells from an aggregate, is affected by many measurement factors including mutual interaction time between cell pairs [21], initial contact area [18,26], and solution properties as the in vitro experimental environment [27]. Experimentally, two individual intact cells were captured by two trapping beams with given power and an initial contact between the cells was formed under the control of the positions of the traps. The contact area was later decreased by slowly moving one trap away from the other until the cell attracting force pulled the RBC out of a trap, or the two cells were separated (contact area decreased to zero) as shown in Fig. 14(a). The average relative linear overlap (l_r) as shown below is used to quantify the extent of contact between two cells:

$$l_r = \left(\frac{x}{d_l} + \frac{x}{d_r}\right) \Big/ 2 \tag{3}$$

where x is the linear distance of overlap between two cells, d_l and d_r are lengths of the left and right RBC. As the cells are deformable and were stretched during the process of disaggregation, the final l_r was calculated using the elongated lengths of RBC denoted as d_l' and d_r' in Fig. 14(a).

Optical pulling force that was able to peel two attached cells to a very small conjugating area was utilized and the effect of laser irradiation was measured in two groups with different initial relative linear overlap. The 4.9 pN and 5.9 pN forces were experimentally selected for the measurement groups of 60% and 80% initial overlap, respectively. The irradiation was performed by a 450-nm laser operated at 5 mW for 5, 15, and 30 min. The percentages of RBC-pairs that were separated from a certain initial overlapping by a given force among at least 10 pairs of tested cells were registered and presented in Fig. 14(b). It can be seen that more cell pairs were successfully detached by a same pulling force from a same initial overlapping after laser irradiation (especially after 15-min irradiation) in comparison with control. In the control sample, only 38% (or 16%) cell pairs with a 60% (or 80%) relative initial contact were separated by the 4.9 pN (or 5.9 pN) pulling force. After 15 min of irradiation (radiant exposure 4.7 J/cm^2), the percentage of separated

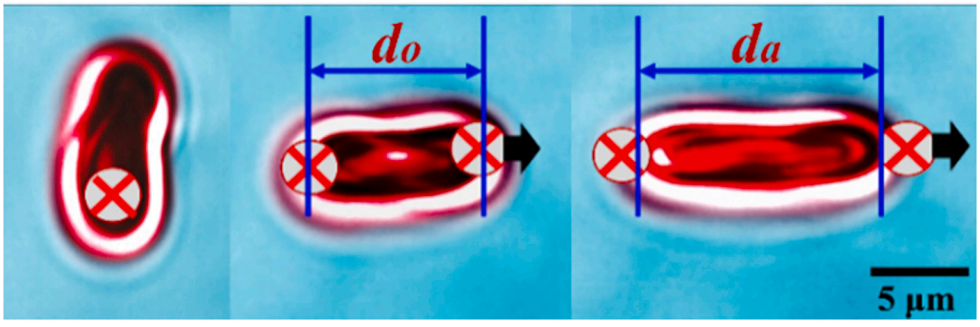

Fig. 12. Schematic diagram of the measurement procedure of cell deformation by dual-trap OT. The circles with red crosses indicate the positions of the traps, the black arrow shows the movement direction of the trap, and d_o and d_a denote the lengths of the trapped cell before and after the stretching action. (For interpretation of the references to colour in this figure legend, the reader is referred to the web version of this article.)

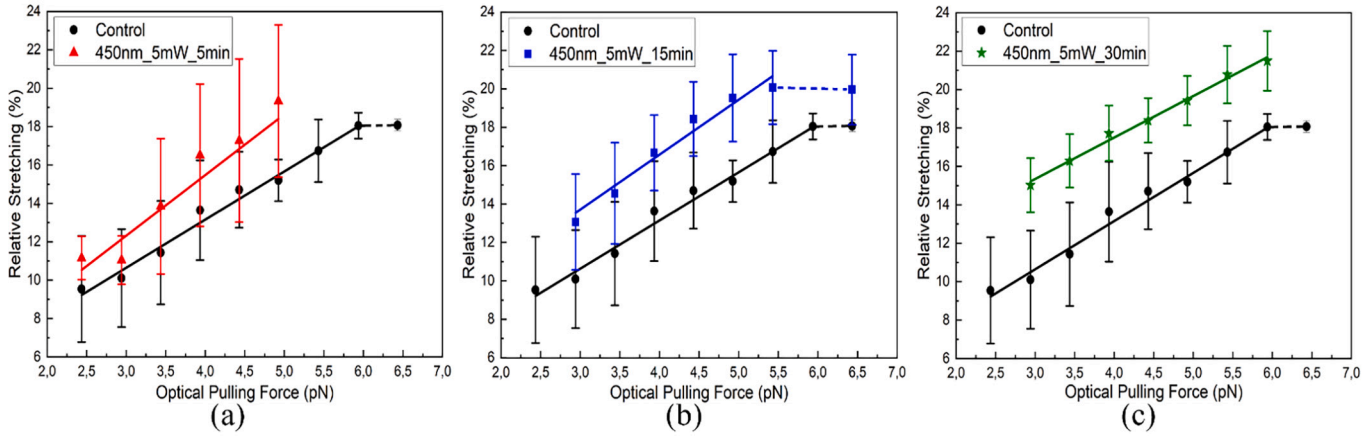

Fig. 13. The comparisons between the results of the cell stretching obtained in the control group (black dots with standard deviations) and in the irradiated groups of (a) "450nm_5mW_5min" (red triangles with standard deviations), (b) "450nm_5mW_15min" (blue squares with standard deviations), and (c) "450nm_5mW_30min" (green stars with standard deviations). The solid lines are linear fitting results, and the dashed lines are used to connect the results when the cell reached its stretching limitation. At least 5 cells were tested by each force. (For interpretation of the references to colour in this figure legend, the reader is referred to the web version of this article.)

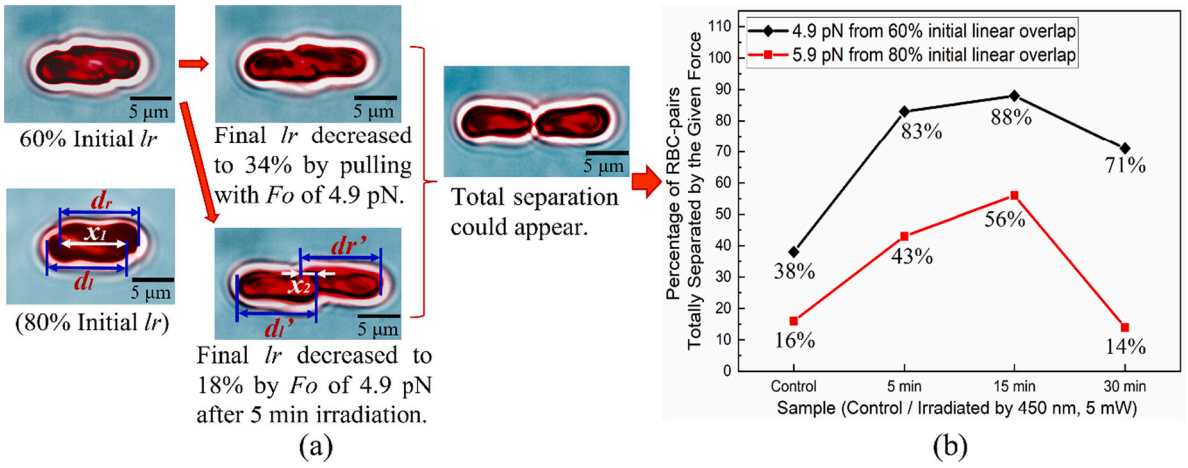

Fig. 14. (a) Illustration of the experimental observation in the RBC disaggregation process. Two cells initially attached by OT (two pictures on the left) were pulled by fixed optical forces at the opposite ends of the cell pair until the cell interaction exceeded the optical force and pulled the cells out of the trapping beam (two pictures in the middle). In some cases, the cell pair can be totally detached (the picture on the right). (b) The percentage of the cases when two cells were completely separated in different conditions of initial overlap (60% and 80%) and with different pulling forces (4.9 pN and 5.9 pN).

cell-pairs increased to 88% (or 56%) by the 4.9 pN (or 5.9 pN) pulling force from a 60% (or 80%) relative initial overlap. The subsequent drop of the value indicates that the optimal irradiation effect occurs within 30-min irradiation (9.5 J/cm^2).

3.5. *Rejuvenating Effect of Laser Irradiation on RBC under Severe Conditions*

An intriguing phenomenon proving the rejuvenating effect of laser irradiation on RBC in terms of keeping the round disc-shapes in the long-stored plasma that was not capable of maintaining the normal shape of RBC in the experimental environment was observed. The suspension of RBC diluted in autologous plasma was injected into two same sample chambers. One served as control and was observed under the 100× water-immersion objective after 0, 5, 15, and 30 min of standing at room temperature. The other was put under the irradiation beam of 450 nm with 5 mW for same time intervals and then observed in the same environment. The image was taken whenever intact disc-shape RBC appeared while moving the sample stage slowly (50 μm/s). When it was too hard to find intact RBC, a photo was taken still after about 10–15 s of searching. 10 photos of each sample were taken and microscopic pictures consisting of 9 photos taken in each group after 0, 15, and 30 min of standing/irradiation time are shown in Fig. 15 to visually demonstrate the effect of laser irradiation on retaining cell state. The total number of intact cells and all objects (an aggregate consisting of several cells was counted as one object) were counted and analyzed as shown in Fig. 16. The percentage of intact cells in both samples was about 31% initially right after the samples were ready. For the irradiated sample, it can be seen that not only the count of intact cells but also the total counts were relatively stable during the first 15 min of irradiation compared to the control sample. The fluctuations in both the percentage of intact cells and the total counts were less than 5% during the first 15 min of irradiation, both dropped only after 30 min of irradiation by 17%. However, the RBC quickly transformed into burr cells (echinocytes) and the cells clumped into large aggregates over time in the control sample. This phenomenon can be easily observed in Fig. 15, the number of intact RBC marked in red was more in the irradiated sample after 15 and 30 min compared to the control sample. Meanwhile, the size of aggregates increased significantly, especially in the picture of 30 min in the control group. Both the analytical results and microscopic photos show that not

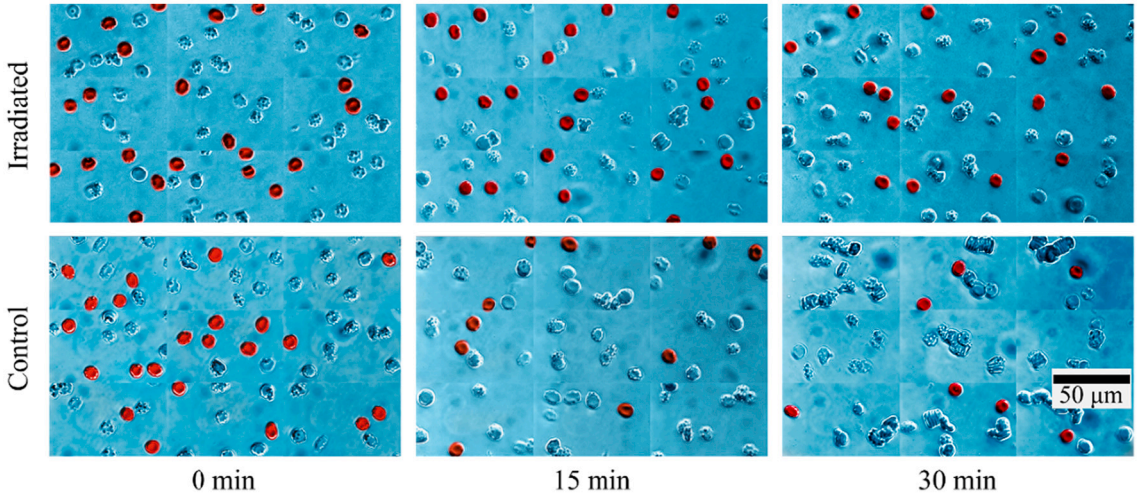

Fig. 15. Colored micrographs consisting of 9 experimental photos taken in the irradiated (by 450-nm laser at 5 mW for up to 30 min) and control samples. The intact cells in round disc shape were colored in red. (For interpretation of the references to colour in this figure legend, the reader is referred to the web version of this article.)

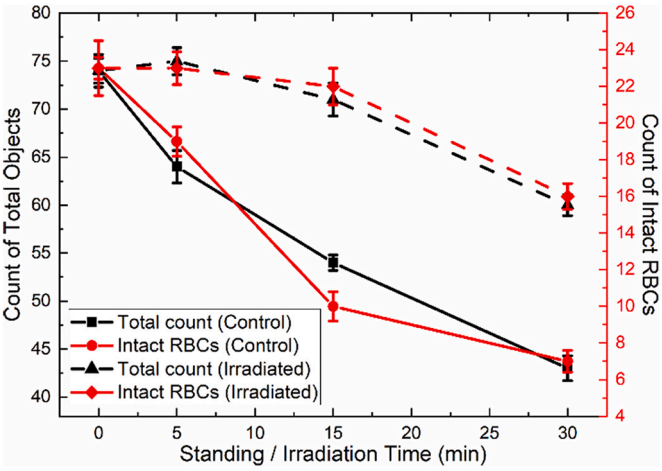

Fig. 16. Counts of all elements (including individual cells and cell-aggregates) and intact RBC with time (up to 30 min) in control and irradiated (by 450-nm laser at 5 mW) samples. The black axis (left) and black line graphs represent the count of all objects, and the red axis (right) and red line graphs represent the count of intact RBC. (For interpretation of the references to colour in this figure legend, the reader is referred to the web version of this article.)

only the cell shape was preserved, but the cell aggregation was also prohibited to some degree by the laser irradiation.

It is important to mention that in normal experimental conditions with the sample preparation method used in this paper, most of the fresh RBC can maintain normal cellular characteristics and shape in relatively fresh plasma (up to two-month storage in the fridge at 1–6 °C) for up to 3 h at room temperature (23 ± 1 °C). Accidently, we noticed that when RBC were suspended in old plasma that has been stored for 5 months, the cells transformed into echinocytes due to changes in the stored plasma (e.g., higher osmolarity [28]). Under such conditions, the rejuvenating or protective effect of laser radiation on RBC is clear. The amplification of laser radiation effects in a defective blood environment agrees well with the results of previous studies [12,29]. It was observed that in blood samples with hyper-viscosity, the irradiation significantly reduced the blood viscosity, though this effect was not observed in normal blood samples [12].

4. Discussion

Hemoglobin is the most abundant biomolecule in the cytoplasm of RBC. It is the iron-containing metalloprotein responsible for oxygen transport and carbon dioxide removal through the circulating of RBC. Hemoglobin is the main absorber of RBC within visible spectral range with absorption peaks at around 400 and 600 nm wavelength [30]. The results of this study show that high-fluence laser irradiation at 450-nm wavelength has a more prominent influence on boosting the formation of aggregates and causing cell morphologic damages compared with 520 nm wavelength at the same radiant fluence. This wavelength-related observation proved that the photon absorption by hemoglobin plays a role in the irradiation process as hemoglobin has a higher absorption coefficient at 450 nm than 520 nm [30].

Studies have found that though hemoglobin can be easily removed from the cell membrane, it is capable of binding to the intracellular surface of normal membranes under certain conditions such as mild oxidative stress [31]. The binding of hemoglobin to the RBC membrane is associated with the flexibility of the RBC by decreasing cell deformability [32]. The hemoglobin-membrane interaction was found to be not affected by temperature variations but dependent on pH value and the ionic composition of the cell environment and impeded by high ionic strength, suggesting the importance of electrostatic bonds in hemoglobin-membrane binding [33,34]. In this study, the deformability of RBC measured by OT was increased by radiant exposure of 4.7 and 9.5 J/cm^2 by 450-nm wavelength. This change in cell deformability is not the result of the thermal effect due to the absorption of radiation because the heat treatment of up to 48 °C has shown to increase membrane viscosity and reduce cell deformability [35]. Therefore, the most possible explanation is that the electromagnetic radiation field interfered with the electrostatic bonds in hemoglobin-membrane interaction in a way that disrupted the binding and led to increased RBC deformability. The change of oxidative stress caused by low-level laser radiation may also play a role in interfering with the hemoglobin-membrane binding as laser radiation has been proved to increase oxidative stress in vitro [36].

RBC aggregation and disaggregation processes have different interaction dynamics and mechanisms. The RBC aggregation follows the “depletion layer” mechanism, which describes the aggregation behavior as the result of osmotic pressure due to the formation of a layer of low macromolecule concentration near the cell surfaces [21,24]. The RBC disaggregation mechanism is more complicated and has been described by the “bridging model” based on the physisorption of macromolecules

(e.g., protein molecules) to cell membranes that connects the adjacent cells [27]. Blood plasma proteins including fibrinogen and albumin is an important determinant in RBC interaction in both aggregation and disaggregation processes [25]. In this study, the spontaneous RBC aggregation was enhanced by laser irradiation with radiant exposure over 9.5 J/cm^2 without influencing the aggregation force. Meanwhile, the LLLR with radiant fluence below 9.5 J/cm^2 was proved to weaken the inter-cell interaction and make RBC aggregates easily separated by an external force. Therefore, it is assumed that the laser radiation did not affect the osmotic pressure in the depletion mechanism but influenced the formation of "cross-bridges" in the bridging model. As the "bridge-formation" process is time-dependent, it is possible that the attachment activity of macromolecules to the surfaces of cell membrane became harder and required longer interaction time due to laser irradiation, making the intercellular interaction measured in a certain cell contact time weaker [18,21]. This assumption is also supported by increased electrophoresis mobility of irradiated blood samples, especially of non-irradiated RBC re-suspended in irradiated plasma, as the weakened attachment of plasma proteins to cell surfaces caused the recovery of the quantity of net negative charges on RBC [12,13].

5. Conclusions

The current study reveals the potential effects of 450 nm and 520 nm laser radiation on rheological properties of RBC at a single-cell level and indicates that LLLR is a potentially effective and non-invasive method in improving blood vitality and microcirculation. It is demonstrated that laser radiation with a high radiant fluence of above 9.5 J/cm^2 by both 450- and 520-nm wavelength speeded up the formation of RBC aggregates, and radiant exposure of over 170.5 J/cm^2 by 450 nm caused irreversible cell morphological changes characterized by increased echinocyte formation. However, the deformability of human RBC was improved and the inter-cell interaction was weakened by the LLLR by wavelength of 450 nm with radiant exposure below 9.5 J/cm^2, while the RBC aggregation force remained unaffected. The underlying mechanism of the observed laser irradiation effects was assumed as the modulations in hemoglobin-membrane binding and macromolecule-membrane interaction induced by photon absorption by hemoglobin and protein molecules in the suspending medium. Further clarification on the bio-modulation mechanism of laser irradiation and the dependence of irradiation effects on the radiant fluence will be the subject of future research. Increased RBC aggregation is a significant manifestation of many pathological processes including ischemic heart disease and is critical in acute clinical conditions such as myocardial/cerebral infarctions [37]. The results will contribute to the development of better treatment of clinical problems involving enhanced RBC aggregation and rigidity in the future.

Funding

This work was funded by China Scholarship Council (CSC No. 201706410089, R.Z.) and the Suomen Kulttuurirahasto (grant No. 00190188, T.A.). The authors also acknowledge the contribution of Russian Science Foundation (project: 19-72-30012) and support from the Academy of Finland (project 325097). I.M. acknowledges the support from the Leverhulme Trust and the Royal Society (Ref. no.: APX111232 APEX Awards 2021). The research was carried out with the support of a grant under the Decree of the Government of the Russian Federation No. 220 of 09 April 2010 (Agreement No. 075-15-2021-615 of 04 June 2021).

CRediT authorship contribution statement

Ruixue Zhu: Conceptualization, Experimental setup preparation, Methodology, Data curation, Writing – original draft, Writing – review & editing. **Tatiana Avsievich:** Conceptualization, Experimental setup preparation, Methodology, Data curation, Writing – review & editing. **Xinyang Su:** Methodology. **Alexander Bykov:** Supervision, Writing – review & editing, Funding acquisition. **Alexey Popov:** Supervision, Writing – review & editing. **Igor Meglinski:** Conceptualization, Supervision, Writing – review & editing, Funding acquisition.

Declaration of Competing Interest

The authors declare no conflict of interest.

References

[1] O.K. Baskurt, B. Neu, H.J. Meiselman, Red Blood Cell Aggregation, CRC Press, 2011, https://doi.org/10.1201/b11221.
[2] R. Zhu, T. Avsievich, A. Popov, I. Meglinski, Optical tweezers in studies of red blood cells, Cells. 9 (2020) 545, https://doi.org/10.3390/cells9030545.
[3] O.K. Baskurt, H.J. Meiselman, Erythrocyte aggregation: basic aspects and clinical importance, Clin. Hemorheol. Microcirc. 53 (2013) 23–37, https://doi.org/10.3233/CH-2012-1573.
[4] A.N. Korolevich, I.V. Meglinsky, Experimental study of the potential use of diffusing wave spectroscopy to investigate the structural characteristics of blood under multiple scattering, Bioelectrochemistry. 52 (2000) 223–227, https://doi.org/10.1016/S0302-4598(00)00109-4.
[5] I.V. Meglinskii, A.N. Korolevich, Use of diffusion wave spectroscopy in diagnostics of blood, J. Appl. Spectrosc. 67 (2000) 709–716, https://doi.org/10.1007/BF02681309.
[6] C. Wagner, P. Steffen, S. Svetina, Aggregation of red blood cells: from rouleaux to clot formation, Comptes Rendus Physique. 14 (2013) 459–469, https://doi.org/10.1016/j.crhy.2013.04.004.
[7] O.K. Baskurt, H.J. Meiselman, RBC aggregation: more important than RBC adhesion to endothelial cells as a determinant of in vivo blood flow in health and disease, Microcirculation. 15 (2008) 585–590, https://doi.org/10.1080/10739680802107447.
[8] D.G. Siposan, A. Lukacs, Effect of low-level laser radiation on some rheological factors in human blood: an in vitro study, J. Clin. Laser Med. Surg. 18 (2000) 185–195, https://doi.org/10.1089/10445470050144038.
[9] J. Zhu, M. Liang, H. Cao, X.-Y. Li, S. Li, S. Li, W. Li, J. Zhang, L. Liu, J. Lai, Effect of intravascular irradiation of he-ne laser on cerebral infarction: Hemorrheology and apoptosis, in: J. Zhu (Ed.), 2004 Shanghai International Conference on Laser Medicine and Surgery, 2005, p. 59671K, https://doi.org/10.1117/12.639329.
[10] N. Ad, U. Oron, Impact of low level laser irradiation on infarct size in the rat following myocardial infarction, Int. J. Cardiol. 80 (2001) 109–116, https://doi.org/10.1016/S0167-5273(01)00503-4.
[11] D.G. Siposan, A. Lukacs, Relative variation to received dose of some Erythrocytic and Leukocytic indices of human blood as a result of low-level laser radiation: an in vitro study, J. Clin. Laser Med. Surg. 19 (2001) 89–103, https://doi.org/10.1089/104454701750285412.
[12] X.Q. Mi, J.Y. Chen, Y. Cen, Z.J. Liang, L.W. Zhou, A comparative study of 632.8 and 532 nm laser irradiation on some rheological factors in human blood in vitro, J. Photochem. Photobiol. B Biol. 74 (2004) 7–12, https://doi.org/10.1016/j.jphotobiol.2004.01.003.
[13] M.S. Al Musawi, M.S. Jaafar, B. Al-Gailani, N.M. Ahmed, F.M. Suhaimi, M. Bakhsh, Erythrocyte sedimentation rate of human blood exposed to low-level laser, Lasers Med. Sci. 31 (2016) 1195–1201, https://doi.org/10.1007/s10103-016-1972-1.
[14] D. Yova, M. Haritou, D. Koutsouris, Antagonistic effects of epinephrine and helium-neon (he-ne) laser irradiation on red blood cells deformability, Clin. Hemorheol. Microcirc. 14 (1994) 369–378, https://doi.org/10.3233/CH-1994-14307.
[15] J.E. Molloy, M.J. Padgett, Lights, action: optical tweezers, Contemp. Phys. 43 (2002) 241–258, https://doi.org/10.1080/00107510110116051.
[16] R. Zhu, T. Avsievich, A. Popov, A. Bykov, I. Meglinski, In vivo nano-biosensing element of red blood cell-mediated delivery, Biosens. Bioelectron. 175 (2021), 112845, https://doi.org/10.1016/j.bios.2020.112845.
[17] T. Avsievich, R. Zhu, A. Popov, A. Bykov, I. Meglinski, The advancement of blood cell research by optical tweezers, Reviews in Physics. 5 (2020), 100043, https://doi.org/10.1016/j.revip.2020.100043.
[18] R. Zhu, T. Avsievich, A. Bykov, A. Popov, I. Meglinski, Influence of pulsed he–ne laser irradiation on the red blood cell interaction studied by optical tweezers, Micromachines. 10 (2019) 853, https://doi.org/10.3390/mi10120853.

[19] T. Avsievich, A. Popov, A. Bykov, I. Meglinski, Mutual interaction of red blood cells influenced by nanoparticles, Sci. Rep. 9 (2019) 5147, https://doi.org/10.1038/s41598-019-41643-x.
[20] Y.Y. Huang, S.K. Sharma, J. Carroll, M.R. Hamblin, Biphasic dose response in low level light therapy–an update, Dose-Response. 9 (2011), https://doi.org/10.2203/dose-response.11-009.Hamblin dose-response.1.
[21] R. Zhu, T. Avsievich, A. Popov, I. Meglinski, Influence of interaction time on the red blood cell (dis)aggregation dynamics in vitro studied by optical tweezers, in: A. Amelink, S.K. Nadkarni (Eds.), Novel Biophotonics Techniques and Applications V, SPIE, 2019, p. 12, https://doi.org/10.1117/12.2526778.
[22] R. Skalak, P.I. Brånemark, Deformation of red blood cells in capillaries, Science. 164 (1969) 717–719, https://doi.org/10.1126/science.164.3880.717.
[23] B. Kaoui, G. Biros, C. Misbah, Why do red blood cells have asymmetric shapes even in a symmetric flow? Phys. Rev. Lett. 103 (2009), 188101 https://doi.org/10.1103/PhysRevLett.103.188101.
[24] T. Avsievich, A. Popov, A. Bykov, I. Meglinski, Mutual interaction of red blood cells assessed by optical tweezers and scanning electron microscopy imaging, Opt. Lett. 43 (2018) 3921, https://doi.org/10.1364/OL.43.003921.
[25] K. Lee, M. Kinnunen, M.D. Khokhlova, E.V. Lyubin, A.V. Priezzhev, I. Meglinski, A. A. Fedyanin, Optical tweezers study of red blood cell aggregation and disaggregation in plasma and protein solutions, J. Biomed. Opt. 21 (2016), 035001, https://doi.org/10.1117/1.JBO.21.3.035001.
[26] R. Zhu, A. Popov, I. Meglinski, Probing the red blood cell interaction in individual cell pairs by optical tweezers, in: Conference on Lasers and Electro-Optics, OSA, Washington, D.C., 2020, p. AW3I.4, https://doi.org/10.1364/CLEO_AT.2020.AW3I.4.
[27] K. Lee, C. Wagner, A.V. Priezzhev, Assessment of the "cross-bridge"-induced interaction of red blood cells by optical trapping combined with microfluidics, J. Biomed. Opt. 22 (2017), 091516, https://doi.org/10.1117/1.JBO.22.9.091516.
[28] J.M. Ratcliffe, M.J. Elliott, R.K. Wyse, S. Hunter, K.G. Alberti, The metabolic load of stored blood. Implications for major transfusions in infants, Arch. Dis. Child. 61 (1986) 1208–1214, https://doi.org/10.1136/adc.61.12.1208.
[29] X.Q. Mi, Y. Chen, Z.J. Liang, L.W. Zhou, In vitro effects of helium-neon laser irradiation on human blood: blood viscosity and deformability of erythrocytes, Photomed. Laser Surg. 22 (2004) 477–482, https://doi.org/10.1089/pho.2004.22.477.
[30] D.J. Faber, E.G. Mik, M.C.G. Aalders, T.G. van Leeuwen, Light absorption of (oxy-) hemoglobin assessed by spectroscopic optical coherence tomography, Opt. Lett. 28 (2003) 1436, https://doi.org/10.1364/OL.28.001436.
[31] E.M. Welbourn, M.T. Wilson, A. Yusof, M.V. Metodiev, C.E. Cooper, The mechanism of formation, structure and physiological relevance of covalent hemoglobin attachment to the erythrocyte membrane, Free Radic. Biol. Med. 103 (2017) 95–106, https://doi.org/10.1016/j.freeradbiomed.2016.12.024.
[32] L.M. Snyder, N.L. Fortier, J. Trainor, J. Jacobs, L. Leb, B. Lubin, D. Chiu, S. Shohet, N. Mohandas, Effect of hydrogen peroxide exposure on normal human erythrocyte deformability, morphology, surface characteristics, and spectrin-hemoglobin cross-linking, J. Clin. Investig. 76 (1985) 1971–1977, https://doi.org/10.1172/JCI112196.
[33] S. Fischer, R.L. Nagel, R.M. Bookchin, E.F. Roth, I. Tellez-Nagel, The binding of hemoglobin to membranes of normal and sickle erythrocytes, Biochimica et Biophysica Acta (BBA) - Biomembranes 375 (1975) 422–433, https://doi.org/10.1016/0005-2736(75)90357-0.
[34] E. Friederichs, H.J. Meiselman, Effects of calcium permeabilization on RBC rheologic behavior, Biorheology. 31 (1994) 207–215, https://doi.org/10.3233/BIR-1994-31208.
[35] G.B. Nash, H.J. Meiselman, Alteration of red cell membrane viscoelasticity by heat treatment: effect on cell deformability and suspension viscosity, Biorheology. 22 (1985) 73–84, https://doi.org/10.3233/BIR-1985-22106.
[36] A. de Souza, G.A. da Fonseca, M. Presta, F. Geller, S.S. Valença Paoli, Low-intensity infrared laser increases plasma proteins and induces oxidative stress in vitro, Lasers Med. Sci. 27 (2012) 211–217, https://doi.org/10.1007/s10103-011-0945-7.
[37] A. Vayá, C. Falcó, E. Réganon, V. Vila, V. Martínez-Sales, D. Corella, T. Contreras, J. Aznar, Influence of plasma and erythrocyte factors on red blood cell aggregation in survivors of acute myocardial infarction, Thromb. Haemost. 91 (2004) 354–359, https://doi.org/10.1160/TH03-08-0497.